The Pom-Pom-Story: From Science Fiction to Reality

Víctor Hugo Rolón-Garrido, Manfred H. Wagner

Polymer Engineering/Polymer Physics, TU Berlin, Fasanenstr. 90, D-10623 Berlin, Germany

ABSTRACT

The pom-pom hypothesis (i.e. side chains are drawn into the backbone tube as soon as the backbone tension equals the number of branches at each end) has never been verified. The Molecular Stress Function model considering: dynamic dilution, finite extensibility, transition from chain stretch to tube squeeze, and dynamics of branch point withdrawal, confirms the hypothesis.

INTRODUCTION

The Doi-Edwards (DE) model[1] is able to describe some rheological phenomena, but its general performance is more qualitative than quantitative. To avoid its limitations, theories accounting for chain stretch have been proposed.

A theory considering chain stretch is the so called Pom-Pom model[2]. The main motivation was to develop a model for predicting simultaneously strain hardening in elongational and shear thinning in shear flow for long-chain-branched polymers like low-density polyethylene (LDPE). The basic topology modeled is a linear backbone with q side chains at each end, i.e. a pom-pom molecule. The original Pom-Pom model[2] was presented in integral form, but the differential approach became much more popular, although it is only a crude approximation of the integral model[3].

In the linear-viscoelastic regime, the basic assumption of the Pom-Pom model is that the side branches relax fast enough to act as un-entangled solvent for the backbone, which then relaxes by reptation.

This is called "dynamic dilution"[4]. In the non-linear deformation regime, the fundamental hypothesis is that the maximum stretch exerted on the backbone is limited by branch point withdrawal, i.e. retraction of the free ends into the original backbone tube as soon as the maximum stretch is equal to the number of dangling arms[2]. The actual occurrence of branch point withdrawal and its significance in the rheology of branched polymers has not been verified so far.

Another widely applied approach, also based on the DE theory, is the Molecular Stress Function (MSF) model[5]. A new version of the MSF model was proposed recently by introducing the interchain pressure term[6] in the evolution equation of the stretch. In this way, the steady-state as well as the transient elongational viscosities of 4 nearly monodisperse polystyrene (PS) melts could be modelled quantitatively by use of a single nonlinear material parameter, the tube diameter relaxation time τ_a[7]. Also, non-Gaussian chain extensibility effects were introduced in the MSF model to describe deviations from the stress optical rule in elongation of two nearly monodisperse PS melts[8].

It remains a challenge to verify model assumptions embedded in constitutive equations by comparison with well-defined and well-characterized model polymers. Recently, elongational viscosity data of a well-defined pom-pom PS melt up to large Hencky strains were presented[9]. It is the aim of the present contribution to analyze these data[9] in the frame of the original integral

version of the Pom-Pom model, and by use of the MSF model with strain-dependent tube diameter, and to elucidate whether the fundamental pom-pom hypothesis, i.e. branch point withdrawal at a relative tension corresponding to the number of arms, is valid or not.

EXPERIMENTAL DATA

The experimental data analyzed are those of Nielsen et al.[9] The polymer sample has a well-defined pom-pom architecture with molecular weight of the backbone M_b and of the arm M_a being *140,000g/mol* and *28,000g/mol*, respectively. Each branch point has an average of *q=2.5* arms. The measurement temperature was 130°C. A discrete relaxation spectrum with partial moduli g_i and relaxation times λ_i was obtained by use of the IRIS program from master curves of *G'* and *G''*. Linear-viscoelastic parameters and molecular characterization are presented in Table I.

THEORY
The Pom-Pom model

The Pom-Pom model version considered here is a multimode approach of the original integral model. Considering only the stress contribution of the backbone, the extra stress tensor is given by

$$\underline{\underline{\sigma}}(t) = \frac{15}{4} \sum_i \lambda_i^2(t) g_i \overline{\underline{\underline{S}}}_i = \frac{15}{4} \sum_i \lambda_i^2(t)\, g_i \bullet$$
$$\bullet \int_{-\infty}^{t} \frac{1}{\tau_i} \exp[-(t-t')/\tau_i] \underline{\underline{S}}_{DE}(t,t') dt \qquad (1)$$

An eight-mode Pom-Pom model is used here. The strain measure $\underline{\underline{S}}_{DE}$ represents the orientation and equilibration of the tube segments and is given by

$$\underline{\underline{S}}_{DE}(t,t') \equiv \frac{1}{\langle u' \rangle} \left\langle \frac{\underline{u}'\underline{u}'}{u'} \right\rangle_o \qquad (2)$$

Table 1. Molecular data and relaxation spectra of pom-pom PS sample at 130 °C

q	2.5
$J_e^0 (Pa^{-1})$	5.190 x10^{-5}
$\eta_0 (Pa.s)$	1.202 x10^8
$Mn,b(kg/mol)$	140
$Mn,a(kg/mol)$	28
g_i [Pa]	τ_i [s]
1.021 x10^7	2.390 x10^{-3}
1.016 x10^5	1.853 x10^0
4.046 x10^5	1.119 x10^{-1}
8.980 x10^4	1.241 x10^1
3.656 x10^4	7.636 x10^1
2.081 x10^4	6.338 x10^2
1.661 x10^4	4.223 x10^3
2.404 x10^3	1.361 x10^4

t is the time of observation, and t' indicates the time of creation of a tube segment. $\underline{u}'\underline{u}'$ is the dyad of a deformed unit vector $\underline{u}'$

$$\underline{u}' = \underline{u}'(t,t') = \underline{\underline{F}}_t^{-1} \cdot \underline{u} \qquad (3)$$

$\underline{\underline{F}}_t^{-1} = \underline{\underline{F}}_t^{-1}(t,t')$ is the relative deformation gradient tensor, and u' is the length of $\underline{u}'$. The orientation average is indicated by

$$\langle ... \rangle_o \equiv \frac{1}{4\pi} \oiint [...] \sin\theta_o d\theta_o d\varphi_o \qquad (4)$$

i.e. an average over an isotropic distribution of unit vectors $\underline{u}$. The pre-factors λ_i represents the backbone stretch of each Pom-Pom mode *i*, governed by the evolution equation

$$\frac{\partial \lambda_i}{\partial t} = \lambda_i \left[\left(\underline{\underline{\kappa}} : \overline{\underline{\underline{S}}}_i \right) - \frac{1}{\tau_{s,i}} \left(\lambda_i - 1 \right) \right]$$
$$\text{strictly for } \lambda_i < q \qquad (5)$$

$\underline{\underline{\kappa}}$ is the velocity gradient and $\tau_{s,i}$ are the stretch relaxation times of each mode, taken as suggested by Inkson et al.[10] as

$$\tau_{s,i} = \frac{1}{2}\tau_i \qquad (6)$$

The maximum value of the backbone stretches λ_i is

$$\lambda_{max,i} = q = 2.5 \qquad (7)$$

The Molecular Stress Function model

The extra stress tensor $\underline{\underline{\sigma}}(t)$ of the MSF model is given by

$$\underline{\underline{\sigma}}(t) = \int_{-\infty}^{t}\sum_{i=1}^{N}\left(\frac{g_i}{\tau_i}\right)e^{\frac{-(t-t')}{\tau_i}} f^2 \underline{\underline{S}}_{DE}^{IA}(t,t')dt' \qquad (8)$$

The molecular stress function $f = f(t,t')$ is inverse proportional to the tube diameter a,

$$f(t,t') = \frac{a_0}{a(t,t')} \qquad (9)$$

representing the relative tension or stretch of tube segments with an equilibrium tube diameter a_0. The strain measure $\underline{\underline{S}}_{DE}^{IA}$ is based on the "independent alignment (IA)" approximation[1] and represents an affine rotation of the tube segments,

$$\underline{\underline{S}}_{DE}^{IA}(t,t') \equiv 5\left\langle\frac{u'u'}{u'^2}\right\rangle_o = 5\underline{\underline{S}}(t,t') \qquad (10)$$

with $\underline{\underline{S}} = \underline{\underline{S}}(t,t')$ being the relative second order orientation tensor.

Comparing Eq.(8) to equation (1), there are three differences: (a) The stretch term is not outside, but inside the integral in Eq. (8). (b) The same stretch is assumed for all relaxation modes. (c) The IA assumption is used in Eq. (8).

As shown by Wagner et al.[7], based on the interchain pressure concept[6], the evolution equation for the tube diameter in elongational flow is given by

$$\frac{\partial f}{\partial t} = f\left[(\underline{\underline{\kappa}}:\underline{\underline{S}}) - \frac{f(f^3-1)}{\tau_a}\right] \qquad (11)$$

with τ_a being the tube diameter relaxation time[7]. In Eq.(11), the first term on the right hand sides describes an on average affine deformation and the second, the interchain pressure contribution.

The MSF model with finite extensibility

With finite chain extensibility effects (FENE), tension f and stretch λ in the chain are different. The MSF model is then given by[8]

$$\underline{\underline{\sigma}}(t) = \int_{-\infty}^{t} m(t-t')f\lambda\,\underline{\underline{S}}_{DE}^{IA}(t,t')dt'. \qquad (12)$$

$\lambda = \lambda(t,t')$ represents now

$$\lambda(t,t') = \frac{a_0}{a(t,t')} = \frac{l(t,t')}{l_0} \qquad (13)$$

with l the deformed and l_0 the equilibrium tube lengths. The FENE effect is implemented in the MSF theory as[8]

$$f = c(\lambda)\lambda \qquad (14)$$

with c a nonlinear spring coefficient, representing a relative Padé approximation[11]

$$c(\lambda) = \frac{\left(3 - \frac{\lambda^2}{\lambda_m^2}\right)\cdot\left(1 - \frac{1}{\lambda_m^2}\right)}{\left(3 - \frac{1}{\lambda_m^2}\right)\cdot\left(1 - \frac{\lambda^2}{\lambda_m^2}\right)} \qquad (15)$$

λ_m is the maximum stretch attainable. For PS a value of $\lambda_m = 5$ is found[8]. The evolution equation with FENE effect is then obtained as[8]

$$\frac{\partial \lambda}{\partial t} = \lambda \left[\left(\underline{\underline{\kappa}} : \underline{\underline{S}} \right) - \frac{1}{\tau_a} \lambda \left(\lambda \, f^2 - 1 \right) \right] \qquad (16)$$

Eq.(16) reduces to Eq.(11) in the Gaussian limit, i.e when $c=1$, and therefore $f=\lambda$.

ANALYSIS OF EXPERIMENTAL DATA

Fig.1 presents the elongational viscosity data[9] for elongation rates of $\dot{\varepsilon}$ from $3 \cdot 10^{-5}$ to $0.1 \mathrm{s}^{-1}$ at 130°C. At smaller elongation rates, the data indicate a steady-state, while at the highest elongation rate, a significant maximum in the elongational viscosity is observed. None of the models discussed so far can explain these maxima. The predictions of the 8-mode Pom-Pom model, Eq.(1)-(7), are also in Fig 1. The start-up of the elongational viscosity is overestimated and the steady-state is significantly underestimated by the Pom-Pom hypothesis of $\lambda_{\max,i} = q = 2.5$.

For the MSF model, and based on arguments preciously proposed[5], the tube diameter relaxation time is related to the maximum tension by[12]

$$\tau_a = \frac{f_{\max} \left(f_{\max}^3 - 1 \right)}{\sqrt{\underline{\underline{D}}^2 : \underline{\underline{S}}}} \qquad (17)$$

leading to an evolution equation of the form

$$\frac{\partial f}{\partial t} = f \left[\left(\underline{\underline{\kappa}} : \underline{\underline{S}} \right) - \frac{f \left(f^3 - 1 \right)}{f_{\max} \left(f_{\max}^3 - 1 \right)} \sqrt{\underline{\underline{D}}^2 : \underline{\underline{S}}} \right] \qquad (18)$$

From the pom-pom hypothesis, $f_{\max}$ is

$$f_{\max} = \frac{a_0}{a_{\min}} = q = 2.5 \qquad (19)$$

$a_{\min}$ is the minimum tube diameter of the backbone. Predictions using Eqs.(8), (18), and (19) are presented in Fig.2.
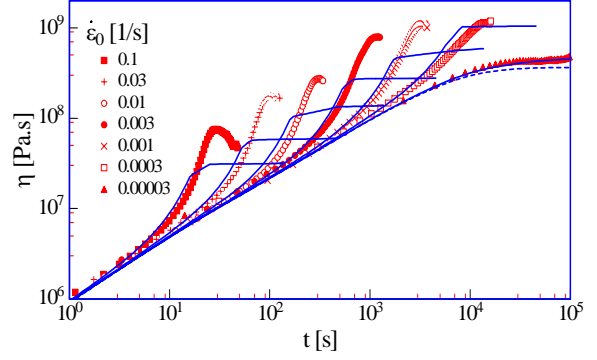

Figure 1. Comparison of measured data to an 8-mode Pom-Pom model.

The start-up of the transient elongational viscosity is now predicted correctly, but the steady-state is still underpredicted.

Dynamic dilution leads to a dilation of the tube diameter, and thereby a reduction in the tension of the backbone chain. Assuming complete relaxation of the pom-pom arms, the remaining weight fraction w of the backbone is

$$w = \frac{M_b}{M_b + 2q \, M_a} = 0.5 \qquad (20)$$

The equilibrium value of the tube diameter a_0 is thereby increased by a factor of $1/w$, resulting in a maximum stretch $f_{\max}$ of
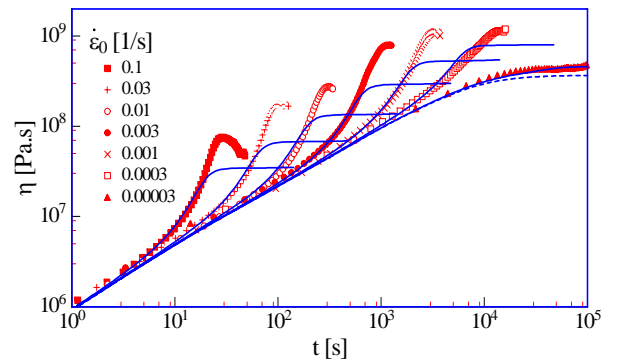

Figure 2. Comparison of measured data to predictions by MSF model.

$$f_{max} = \frac{a_0 / w}{a_{min}} = q / w = 5 \qquad (21)$$

The relative tension in the backbone must increase by a factor of 5 relative to its equilibrium tension before the dangling side chains are drawn into the tube of the backbone. Predictions of the MSF model with Eqs.(8), (18), and (21) are presented in Fig.3. Agreement is improved with the dynamic dilution effect, although the maxima are now slightly overpredicted.

So far, Gaussian chain statistics has been assumed. However, the maximum extensibility λ_m of the backbone even taking into account the dilution effect is only

$$\lambda_m = 0.82 \sqrt{\frac{M_e / M_0}{C_\infty w}} = \frac{5}{\sqrt{w}} \approx 7 \qquad (22)$$

which is of the same order of magnitude as the maximum relative tension $f_{max} = 5$. Thus, finite extensibility must be used. From Eqs.(14) and (15), for a tension of $f_{max} = 5$, a relative stretch of $\lambda_{max} = 3.91$ is found. With τ_a in Eq.(16) given as

$$\tau_a = \frac{\lambda_{max} \left(\lambda_{max} f_{max}^2 - 1 \right)}{\sqrt{\underline{\underline{D}}^2 : \underline{\underline{S}}}} \qquad (23)$$
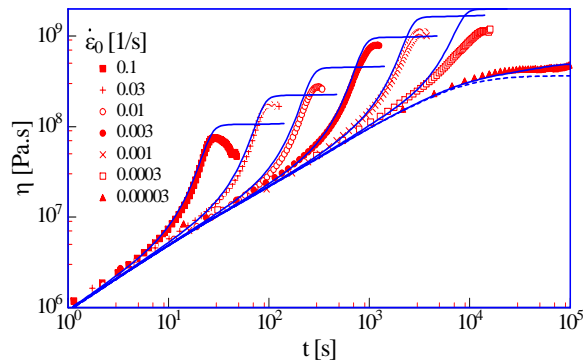

Figure 3. Comparison of measured data to predictions by MSF model considering dynamic dilution.
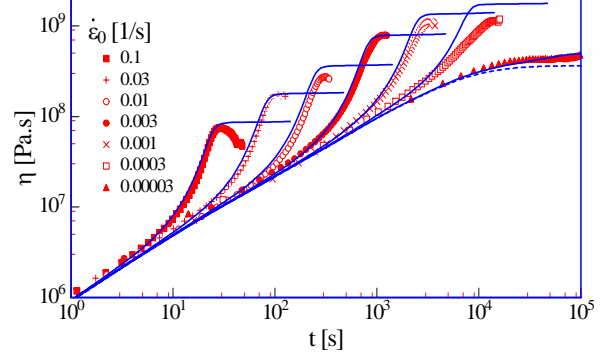
Figure 4. Comparison of measured data to predictions by MSF model considering dynamic dilution and finite extensibility.

the evolution Eq.(16) takes the form

$$\frac{\partial \lambda}{\partial t} = \lambda \left[\left(\underline{\underline{\kappa}} : \underline{\underline{S}} \right) - \frac{\lambda \left(\lambda f^2 - 1 \right)}{\lambda_{max} \left(\lambda_{max} f_{max}^2 - 1 \right)} \sqrt{\underline{\underline{D}}^2 : \underline{\underline{S}}} \right] \qquad (24)$$

Predictions of the MSF model with FENE are presented in Fig. 4. Note that perfect agreement at the higher elongation rates and up to the maximum of the elongational viscosity is achieved without any free parameters of the model, but is solely based on the molecular quantities q and w defined by the structure considered.

Predictions for smaller elongation rates can be improved by considering a cross-over from affine stretch to tube squeeze[13], which leads to an evolution equation of the form

$$\frac{\partial \lambda}{\partial t} = \lambda \left[\left(\underline{\underline{\kappa}} : \underline{\underline{S}} \right) - \frac{1}{\tau_s} \frac{f - 1}{\lambda} - \frac{1}{\tau_a} \lambda \left(\lambda f^2 - 1 \right) \right] \qquad (25)$$

As seen in Fig.5, with τ_a from Eq.(23) and a value of the stretch relaxation time of $\tau_s = 5000s$, good agreement between experimental data and model up to the maximum of the elongational viscosity is achieved for all deformation rates measured.

It is obvious from Fig.5 that the maximum in the elongational viscosity is

reached when the tension in the backbone is as high as the combined tension of the q
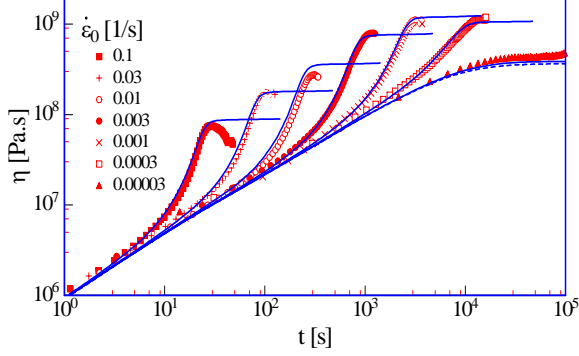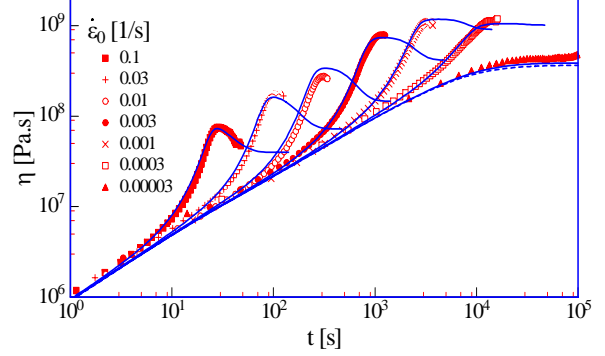

Figure 5. Comparison of measured data to predictions by MSF model considering dynamic dilution, FENE and cross-over from affine stretch to tube squeeze.

dangling arms, and the dangling arms are drawn into the tube of the backbone.

As a possible explanation for the maximum in the elongational viscosity we advance the hypothesis that when the dangling arms are drawn into the tube of the backbone, they loose their character as individually entangled side chains and behave as a single entity, thereby elongating the backbone on each side by a length equivalent to M_a. After the maximum, the pom-pom melt will therefore transit to a deformation behavior as observed in the case of a monodisperse linear melt with molar mass $M_b+2M_a=196,000$g/mol. A melt of this molar mass is expected to show a constant tube diameter relaxation time τ_a, which can be estimated from Wagner et al.[7] as $\tau_a = 270s$ at 130°C. As a possible cross-over function we propose

$$\tau_a = 270s + \frac{\lambda_{max}\left(\lambda_{max} f_{max}^2 - 1\right)}{\sqrt{\underline{\underline{D}}^2 : \underline{\underline{S}}}} \bullet$$
$$\bullet \frac{1}{1 + \tau_r \sqrt{\underline{\underline{D}}^2 : \underline{\underline{S}}}\left(e^{<\ln u'>} - \lambda\right)} \tag{26}$$

This is motivated by the fact that $\lambda = e^{<\ln u'>}$ as long as the stretch is affine, while when λ reaches its maximum value and then starts to decrease, $e^{<\ln u'>}$ still

Figure 6. Comparison of measured data to predictions by MSF model considering considering dynamic dilution, FENE, cross-over from affine stretch to tube squeeze and backbone extension.

increases. For a value of $\tau_r = 2s$, excellent agreement between experimental data and predictions of Eqs.(13), (17), and (26) is obtained as seen in Fig.6. It should be mentioned that τ_r is of the order of the stretch relaxation time of the dangling arms as reported by Nielson et al.[9].

CONCLUSIONS

The fundamental pom-pom hypothesis, i.e. the retraction of the q side chains into the tube of the backbone starts as soon as the relative tension in the backbone reaches a value of q, is confirmed here for the first time.

To achieve quantitative agreement between experiment and modelling, it is essential to assume a time- and strain-dependent tube diameter, and to place the expressions of stretch and tension inside the integral. The equilibrium tube diameter of the backbone increases by dynamic dilution of the backbone due to the relaxation of the dangling arms. This reduces the equilibrium tension in the backbone and has a crucial impact on the force equilibrium at the branch points. The relative tension which is needed for branch point withdrawal is

increased by this effect by a factor which is inverse proportional to the weight fraction of the backbone.

To get quantitative agreement between experiment and model, FENE effects have to be taken into account, and the difference between relative tension and relative stretch has to be considered.

At lower strain rates, a transition from affine chain stretch to tube squeeze is observed, i.e. the stretch is no longer affine with the macroscopic stretch, but is caused by an affine reduction of the tube diameter.

The maximum observed in the elongational viscosity may be explained by the hypothesis that when the dangling arms are drawn into the tube of the backbone, they loose their character as individually entangled side chains, and the macromolecule behaves as a single linear entity.

REFERENCES
1. Doi, M and Edwards S.F. (1986), "Theory of Polymer Dynamics", Oxford University Press, Great Britain.
2. McLeish, T.C.B. and Larson R.G. (1998), "Molecular constitutive equations for a class of branched polymers: The pom-pom polymer", J. Rheol. 42(1), 81-110.
3. Rubio, P. and Wagner M.H. (2000), "LDPE melt rheology and the pom-pom model", J. Non-Newtonian Fluid Mech. 92, 245-259.
4. Ball, R.C. and McLeish T.C.B. (1989), "Dynamic Dilution and the Viscosity of Star Polymer Melts", Macromolecules 22, 1911-1913.
5. Wagner. M.H., Rubio P. and Bastian H. (2001), "The molecular stress function model for polydisperse polymer melts with dissipative convective constraint release", J. Rheol. 45(6), 1387-1412.
6. Marrucci, G. and Ianniruberto G. (2004), "Interchain Pressure Effect in Extensional Flows of Entangled Polymer Melts", Macromolecules 37, 3934-3942.
7. Wagner, M.H., Kheirandish S, Hassager O (2005), "Quantitative Prediction of Transient and Steady-State Elongational Viscosity of Nearly Monodisperse Polystyrene Melts", J. Rheol. 49, 1317-1327.
8. Rolón-Garrido, V.H., Wagner M.H., Luap C. and Schweizer T. (2006), "Modeling Non-Gaussian Extensibility Effects in Elongation of Nearly Monodisperse Polystyrene Melts", J. Rheol. 50, 327-340.
9. Nielsen, J.K., Rasmussen H.K., Denberg M., Almdal K. and Hassager O. (2006), "Nonlinear branch-point dynamics of multiarm polystyrene", Macromolecules 39, 8844-8853.
10. Inkson, N.J., McLeish T.C.B., Harlen O.G. and Groves D.J. (1999), "Predicting low density polyethylene melt Rheology in elongational and shear flows with "pom-pom" constitutive equations", J. Rheol. 43(4), 873-896.
11. Ye, X. and Sridhar T. (2005), "Effects of the Polydispersity on Rheological Properties of Entangled Polystyrene Solutions", Macromolecules 38, 3442-3449.
12. Rolón-Garrido, V.H. and Wagner M.H. (On line), "The MSF model: relation of nonlinear parameters to molecular structure of long-chain branched polymer melts", Rheol.ActaDOI10.1007/s00397-006-0136-9.
13. Wagner, M.H., Bastian H., Hachmann P., Meissner J., Kurzbeck S., Münstedt H., Langouche F. (2000), "The strain-hardening behaviour of linear and long-chain-branched polyolefin melts in extensional flows", Rheol. Acta 39, 97-109.